

Effective dark matter-standard model interactions with spin-one mediators

Fabiola Elena Fortuna Montecillo

Work done in collaboration with Pablo Roig

e-Print: 2208.12330 [hep-ph]

CINVESTAV

XVIII Mexican Workshop on Particles and Fields

November 2022



Outline

Motivation

Effective Field Theory

Lagrangian

Observational limits

Direct Detection Experiments

Limits from dwarf spheroidal satellite galaxies (dSphs)

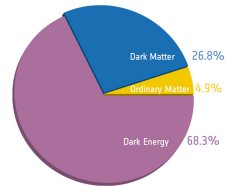
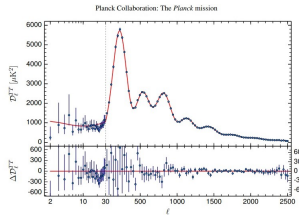
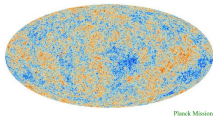
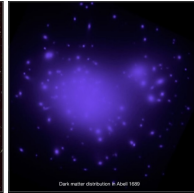
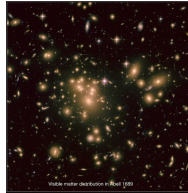
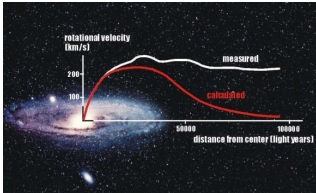
Limits from AMS-02 positron measurements

Collider constraints

Results



Evidence for dark matter is abundant and compelling



Effective Field Theory

- DM-SM interaction.¹
- Heavy mediators that can be scalars, fermions or **vectors**.
- Dark sector:
 - ▶ Scalars Φ
 - ▶ Fermions Ψ
 - ▶ Vectors X
- The mediators are weakly coupled to both sectors, dark and standard.
- The dark fields transform non-trivially under \mathcal{G}_{DM} .
- All SM particles are singlets under $\mathcal{G}_{\text{DM}} \rightarrow$ stable DM particle.
- All dark fields are singlets under $\mathcal{G}_{\text{SM}} = SU(3) \otimes SU(2) \otimes U(1)$.
- The consequence of interactions generated by a mediator are:

$$\mathcal{O} = \mathcal{O}_{\text{SM}} \mathcal{O}_{\text{dark}} \quad (1)$$

- In the effective lagrangian, each term has a factor $1/\Lambda^n$, $n = \dim(\mathcal{O}) - 4$.
- As we assume that the dark fields transform non-trivially under \mathcal{G}_{DM} , we know that $\mathcal{O}_{\text{dark}}$ contains at least two fields.

¹González-Macías & Wudka *JHEP* 1507 (2015) 161. Follow-up work:
González-Macías et al. *JHEP* 05 (2016) 171 and
Lamprea et al. *Phys.Rev.D* 103 (2021) 1, 015017.



- Terms with dark fermions (Ψ):

$$\begin{aligned}\mathcal{L}_{\text{eff}}^{\Psi} = & \frac{\Upsilon_{\text{eff}}}{\Lambda} B_{\mu\nu} \bar{\Psi} \sigma^{\mu\nu} \Psi + \frac{A_{\text{eff}}^{L,R}}{\Lambda^2} \bar{\psi} \gamma_{\mu} \psi \bar{\Psi} \gamma^{\mu} P_{L,R} \Psi \\ & + \frac{\kappa_{\text{eff}}^{L,R}}{\Lambda^2} B_{\mu\nu} \bar{\Psi} (\gamma^{\mu} \overleftrightarrow{\mathcal{D}}^{\nu} - \gamma^{\nu} \overleftrightarrow{\mathcal{D}}^{\mu}) P_{L,R} \Psi.\end{aligned}\quad (2)$$

- Terms with dark bosons (X, Φ):

$$\mathcal{L}_{\text{eff}}^{\Phi, X} = \frac{\zeta_{\text{eff}}}{\Lambda} B_{\mu\nu} X^{\mu\nu} \Phi + \frac{\epsilon_{\text{eff}}}{\Lambda^2} \bar{\psi} \gamma_{\mu} \psi \frac{1}{2i} \Phi^{\dagger} \overleftrightarrow{\mathcal{D}}^{\mu} \Phi. \quad (3)$$

Where

$$B = A \cos \theta - Z \sin \theta. \quad (4)$$

Observational limits

We introduce the following notation that we will use below:

$$\begin{aligned} \text{OP1} &\equiv B_{\mu\nu} \bar{\Psi} \sigma^{\mu\nu} \Psi, \\ \text{OP2} &\equiv \bar{\psi} \gamma^\mu \psi \bar{\Psi} \gamma_\mu P_{L,R} \Psi, \\ \text{OP3} &\equiv B_{\mu\nu} \bar{\Psi} (\gamma^\mu \overleftrightarrow{D}^\nu - \gamma^\nu \overleftrightarrow{D}^\mu) P_{L,R} \Psi, \\ \text{OP4} &\equiv B_{\mu\nu} X^{\mu\nu} \Phi, \\ \text{OP5} &\equiv \frac{1}{2i} (\bar{\psi} \gamma^\mu \psi) \left(\Phi^\dagger \overleftrightarrow{\partial}_\mu \Phi \right). \end{aligned} \quad (5)$$

Besides, we use the effective couplings that correctly reproduce the observed relic abundance.

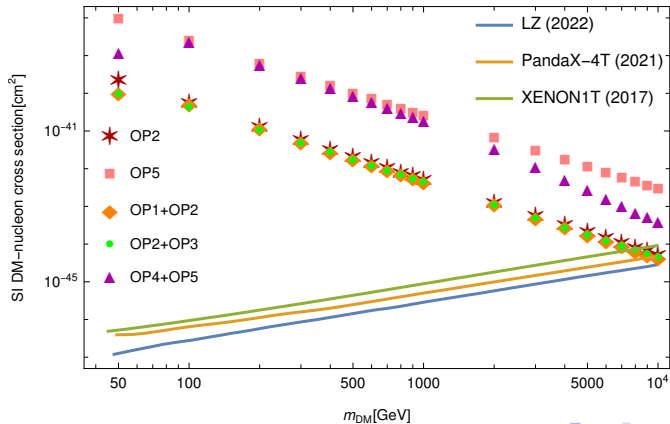
We also analyze the combined contributions with the same DM candidate, with the following relations between the Λ scales and the C coefficients of the operators:

$$\Lambda_{\text{dim } 6} = \Lambda_{\text{dim } 5}, \quad C_{\text{dim } 6} = \pm C_{\text{dim } 5}. \quad (6)$$



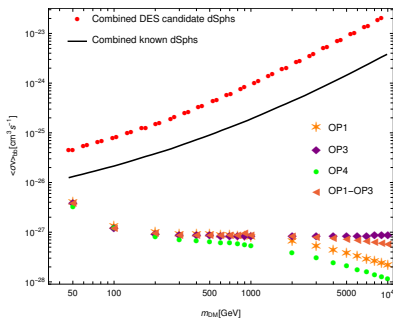
Direct Detection Experiments

Currently the most stringent limit on spin-independent scattering cross sections of DM-nucleon come from the LUX-ZEPLIN, PandaX-4T and XENON1T. We study DM-nucleon cross sections in the limit where the relative velocity goes to zero, using micrOMEGAs.

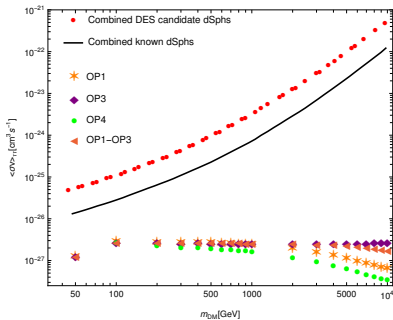


Limits from dwarf spheroidal satellite galaxies (dSphs)

The dwarf spheroidal satellite galaxies (dSphs) of the Milky Way are some of the most DM dominated objects known. Drlica-Wagner et al. ² searched for gamma-ray emission coincident with the positions of the dSphs in six years of Fermi Large Area Telescope data and no significant excesses of gamma-ray emission were found.



(a) Annihilation to $b\bar{b}$



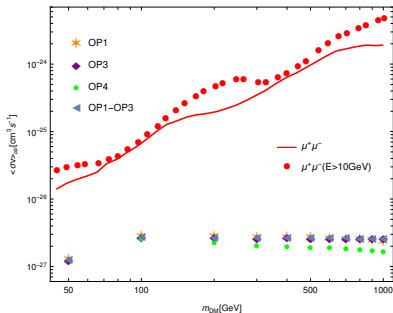
(b) Annihilation to $\tau^+\tau^-$

²A. Drlica-Wagner et al. Search for Gamma-Ray Emission from DES Dwarf Spheroidal Galaxy Candidates with Fermi-LAT Data. *Astrophys. J.* **809(1)**:L4, 2015

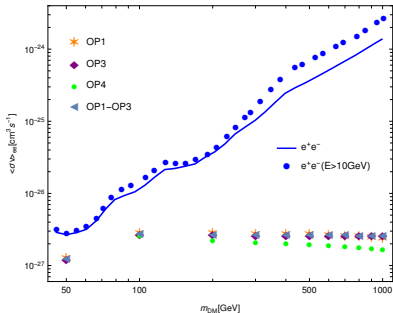


Limits from AMS-02 positron measurements

Ibarra, Lamperstorfer and Silk³ used measurements of the positron flux to derive limits on the dark matter annihilation cross section and lifetime for various final states, and extracted strong limits on DM properties.



(a) Annihilation to $\mu^+\mu^-$



(b) Annihilation to e^+e^-

³Alejandro Ibarra, Anna S. Lamperstorfer, and Joseph Silk. Dark matter annihilations and decays after the AMS-02 positron measurements. *Phys. Rev. D* 89(6):063539, 2014.



Collider constraints

The effective operators we are working with allow for the pair production of WIMPs (χ) in the proton-proton collisions at the LHC. If one of the incoming partons radiates a jet through initial state radiation (ISR), one can observe the process $pp \rightarrow \chi\chi j$ as a single jet associated with missing transverse energy (E_T). In this study, we include the ATLAS ⁴ monojet analysis based on 139 fb^{-1} of data from Run II.

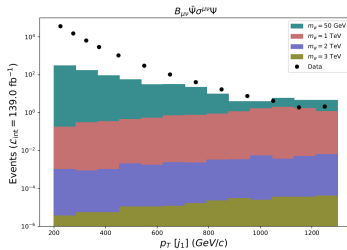
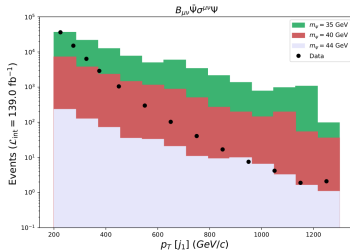
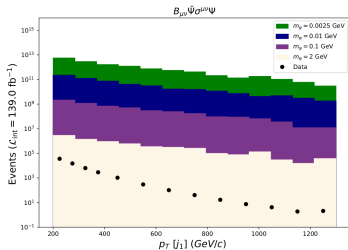
Operator	Dim.	DM candidate	Allowed mass (GeV) ⁵
1.- $B_{\mu\nu} \bar{\Psi} \sigma^{\mu\nu} \Psi$	5	Ψ fermion	$\approx 0.0025 - 2, \approx 33 - 44.5$
2.- $\bar{\psi} \gamma_\mu \psi \bar{\Psi} \gamma^\mu P_{L,R} \Psi$	6	Ψ fermion	none
3.- $B_{\mu\nu} \bar{\Psi} (\gamma^\mu \overleftrightarrow{D}^\nu - \gamma^\nu \overleftrightarrow{D}^\mu) P_{L,R} \Psi$	6	Ψ fermion	$\approx 33 - 44.5$
4.- $B_{\mu\nu} X^{\mu\nu} \Phi$	5	vector X , scalar Φ	$\approx 0.11 - 2, \approx 36 - 44.5$
5.- $\bar{\psi} \gamma_\mu \psi \frac{1}{2i} \Phi^\dagger \overleftrightarrow{D}^\mu \Phi$	6	scalar Φ	none
1 + 2	5+6	Ψ fermion	$\approx 0.0025 - 2$
1 + 3	5+6	Ψ fermion	$\approx 0.0025 - 2, \approx 33 - 44.5$
2 + 3	6	Ψ fermion	none

⁴ Georges Aad et al. *Phys. Rev. D*, 103(11):112006, 2021.

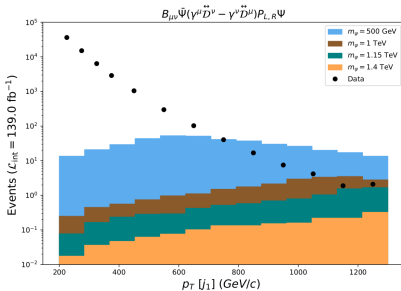
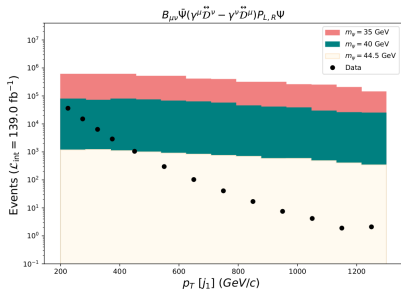
⁵ Fortuna, Roig and Wudka. *JHEP* 02(2021) 223.



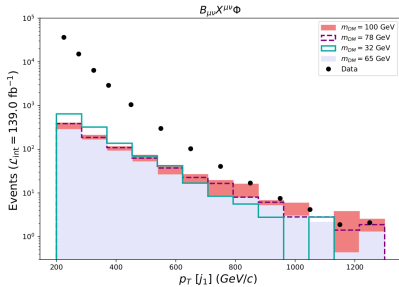
Collider constraints. OP1



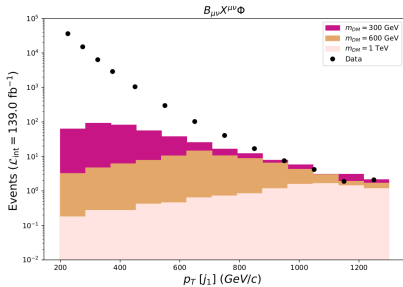
Collider constraints. OP3



Collider constraints. OP4



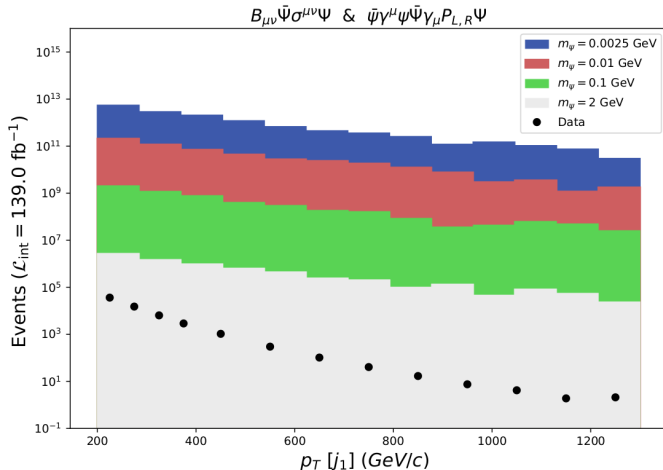
(a)



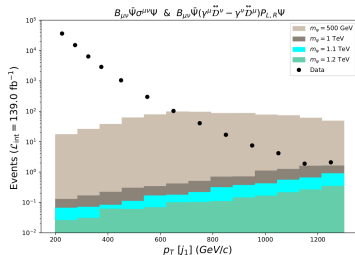
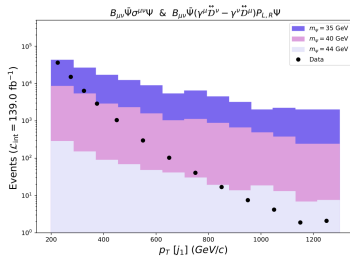
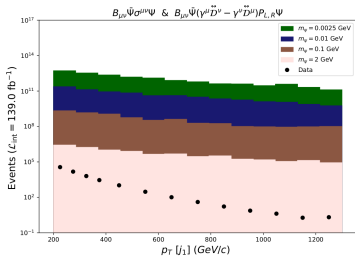
(b)



Collider constraints. OP1 & OP2



Collider constraints. OP1 & OP3



Summary of results

We recall that the effective coefficients are the ones that correctly reproduce the relic abundance.

Operator	Dim.	DM candidate	Allowed mass (GeV) ⁶
1.- $B_{\mu\nu}\bar{\Psi}\sigma^{\mu\nu}\Psi$	5	Ψ fermion	> 1000
2.- $(\bar{\psi}\gamma_{\mu}\psi)(\bar{\Psi}\gamma^{\mu}P_{L,R}\Psi)$	6	Ψ fermion	none
3.- $B_{\mu\nu}\bar{\Psi}(\gamma^{\mu}\overleftrightarrow{D}^{\nu} - \gamma^{\nu}\overleftrightarrow{D}^{\mu})P_{L,R}\Psi$	6	Ψ fermion	> 1150
4.- $B_{\mu\nu}X^{\mu\nu}\Phi$	5	vector X , scalar Φ	$[32, 78] \ \& \ > 600$
5.- $(\bar{\psi}\gamma_{\mu}\psi)\frac{1}{2i}\Phi^{\dagger}\overleftrightarrow{D}^{\mu}\Phi$	6	scalar Φ	none
1 ± 2	5+6	Ψ fermion	none
$1 + 3$	5+6	Ψ fermion	> 1000
$1 - 3$	5+6	Ψ fermion	> 1100
2 ± 3	6	Ψ fermion	none

⁶e-Print: 2208.12330 [hep-ph]



Thank you

